CHEMBIOCHEM

DOI: 10.1002/cbic.201100414

Dynamic Substrate Enhancement for the Identification of Specific, Second-Site-Binding Fragments Targeting a Set of Protein Tyrosine Phosphatases

Marco F. Schmidt,[b, c, e] Matthew R. Groves,[d] and Jörg Rademann*[a, b]

Protein tyrosine phosphatases (PTPs) are key regulators in living systems and thus are attractive drug targets. The development of potent, selective PTP inhibitors has been a difficult challenge mainly due to the high homology of the phosphotyrosine substrate pockets. Here, a strategy of dynamic substrate enhancement is described targeting the secondary binding sites of PTPs. By screening four different PTPs from bacterial (MptpA) and human origin (PTP1B, HePtp, Shp2) with this assay, specific fragments were identified. One highly specific fragment that binds to the secondary site of *Mycobacterium tuberculosis* protein tyrosine phosphatase A (MptpA) was characterized in order to validate the assay concept. Finally by covalently linking the secondary fragment to a phosphotyrosine mimetic, a moderately active but highly specific inhibitor of MptpA was obtained.

Introduction

Protein tyrosine phosphorylation plays a central role in living systems as the dominant on/off switch of protein function. Tyrosine phosphorylation is both dynamic and tightly regulated, controlled by the opposing actions of protein tyrosine kinases (PTKs) and protein tyrosine phosphatases (PTPs).[1] Several PTKs and PTPs have been identified as attractive therapeutic targets in human diseases including autoimmunity, obesity, diabetes, and cancer.[2,3] Potent PTK inhibitors have been developed and are used successfully in the clinic.[4] On the other hand, the development of potent, selective PTP inhibitors remains a difficult task mainly due to the high homology of the catalytic domains of PTPs.[5–7] In addition, the active sites of PTPs are smaller than those of PTKs and highly charged, thus posing additional challenges for the development of potent inhibitors with good pharmacokinetic properties. Recently, Knapp's group compared the crystal structures of 22 human PTPs and concluded that protein pockets next to the active sites are less homologous among PTPs.[8] Exploiting these "secondary binding sites" might offer new opportunities to identify specific PTP inhibitors.

Classically, small molecular entities that bind to secondary binding sites were identified by biophysical fragment screening.[9] With either NMR spectroscopy or X-ray crystallography for detection, this approach is capable of identifying low-affinity fragments that bind to a defined site. It does not, however, provide sufficient information on how to convert low-affinity hit fragments into specific inhibitors. Moreover, the biophysical methods require expensive equipment and are operated with low throughput.[10]

In this contribution, a concept is established that exploits the screening of enzyme substrates generated by dynamic fragment ligation for the development of second-site-selective inhibitors. We propose the term "dynamic substrate enhancement" for this method in order to describe its characteristics. This method employs a generic PTP substrate carrying an aldehyde functionality that enables dynamic, template-assisted ligation with nucleophiles. With this setup fragments recognized specifically by the secondary binding site of the enzyme should be identified by a significantly enhanced turnover of the generic substrate.

This novel methodology builds on the recently established concept of dynamic ligation screening (DLS). DLS has been used to identify fragments in a high-throughput assay either through enhancing the inhibition of a fluorogenic substrate,[11] or enhancing binding as detected in an anisotropy (fluorescence-polarization) assay.[12] In addition, dynamic substrate enhancement, as demonstrated here, supports the recent finding of Ellman's group that screening substrate libraries can be useful for the development of improved enzyme inhibitors.[13]

[a] *Prof. Dr. J. Rademann*
Medicinal Chemistry, Institute of Pharmacy, Leipzig University
Brüderstrasse 34, 04103 Leipzig (Germany)
E-mail: rademann@uni-leipzig.de

[b] *Dr. M. F. Schmidt, Prof. Dr. J. Rademann*
Leibniz-Institut für Molekulare Pharmakologie (FMP)
Robert-Rössle-Strasse 10, 13125 Berlin (Germany)

[c] *Dr. M. F. Schmidt*
Institute of Chemistry and Biochemistry, Freie Universität Berlin
Takustrasse 3, 14195 Berlin (Germany)

[d] *Dr. M. R. Groves*
European Molecular Biology Laboratory (EMBL)
Notkestrasse 85, 22603 Hamburg (Germany)

[e] *Dr. M. F. Schmidt*
Current address:
University Chemical Laboratory, University of Cambridge
Lensfield Road, Cambridge, CB2 1EW (UK)

Results and Discussion

A generic PTP substrate, 4-(formyl)phenylphosphate (**1**), which contains an aldehyde group, was investigated as a dynamic ligation probe. The *O*-aryl phosphate could be hydrolyzed by the catalytic active sites of all tested PTPs. For dynamic substrate enhancement, substrate **1** was incubated with an excess of one amine fragment per well and the PTP of interest. After a fixed time, the enzymatic reaction was terminated, and the released phosphate (P_i) was quantified as the green ammonium phosphomolybdate complex of Malachite Green at 630 nm (Figure 1).[14] In agreement with our recent work on caspase-3,[12] three outcomes of this experiment are conceivable. A) The

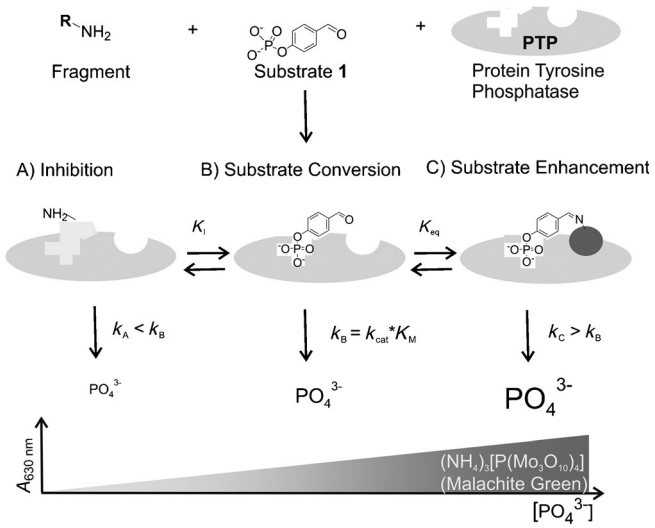

Figure 1. Differential detection of cooperatively binding or inhibitory nucleophilic fragments R–NH_2 in one dynamic substrate-ligation assay of PTPs. The turnover of substrate **1** can be monitored by measuring the Malachite Green phosphomolybdate complex formed from released phosphate anion (P_i). Three alternative scenarios of fragment interactions can be distinguished in the assay. A) (Inhibition) binding of fragment R–NH_2 leads to decreased phosphate formation. B) In contrast, nonbinding R–NH_2 fragments have no effect on substrate conversion or the formation of the Malachite Green complex. C) Cooperative binding of the nucleophilic fragment and substrate **1** to the protein results in enhanced substrate turnover by the PTP and thus increased the phosphate signal.

quantity of P_i is decreased; this would suggest that the tested fragment acts as an inhibitor of the PTP. B) No change in the P_i concentration is observed; this would indicate no binding of the amine. C) The observed P_i concentration increases; this would indicate enhanced activity of substrate **1**, presumably by ligation of the fragment. Accordingly, it should be possible to identify competitive inhibitors and cooperatively binding, substrate-enhancing fragments in one primary screen.

To demonstrate the approach, we selected a set of therapeutically relevant PTPs: *Mycobacterium tuberculosis* protein tyrosine phosphatase A (MptpA), protein tyrosine phosphatase 1B (PTP1B), protein tyrosine phosphatase N7 (PTPN7 also known as HePTP for hematopoietic PTP), and protein tyrosine phosphatase 11 (PTPN11 also known as Shp2). MptpA is believed to mediate *M. tuberculosis* survival in host cells.[15] PTP1B acts as a negative regulator of insulin and is therefore an attractive target for the treatment of type II diabetes and obesity.[16] HePTP (PTPN7) has been shown to be over-expressed in some patients with acute myeloblastic leukemia, thus suggesting a link between increased HePTP activity and this disease.[17] Finally, activating mutations in Shp2 (PTPN11) cause Noonan syndrome and have been identified in human cancer. In addition, Shp2 is under consideration as a drug target against cancer-cell metastasis.[18]

Initially, substrate **1** was assayed against every PTP in 50 mM Tris·HCl (pH 7.0) in order to determine the K_M values and to optimize enzyme concentrations and incubation times (see the Experimental Section). The conventional addition of dithiothreitol (DTT) to the buffer was avoided in order to exclude any interaction of the dithiol with the aldehyde electrophile. For the dynamic substrate-enhancement assay, a concentration of 250 μM of **1** was selected. A diverse set of 110 fragments (primary amines) was assembled[19] and screened at a concentration of 500 μM against each PTP. In the case of MptpA, two enhancing fragments and one potent competitive inhibitor were identified; for PTPN7, six enhancing molecules and one potent competitive inhibitor were observed; seven enhancing binders and one potent competitive inhibitor were found to be active in the case of PTPN11; while two amines enhanced the activity of PTP1B and one amine showed total inhibition of PTP1B. The identified enhancing binders were structurally diverse (Scheme 1); all but one only displayed enhancing effects against a single PTP. As a control, all hit fragments were tested against their target PTPs without substrate **1** in the established *p*NPP and DiFMUP assays.[20] None of the enhancing fragments increased substrate turnover by PTP alone, thereby excluding the possibility of allosteric activation and supporting the postulated substrate enhancement by template-assisted ligation. On the other hand, the identified competitive inhibitor **2** was active towards all tested PTPs, and similar 2,4-thiazolidinones have been recently described as PTP inhibitors.[21] According to our results, compound **2** is an unselective and competitive PTP inhibitor—K_I values have been determined for the four PTPs (Scheme 1). Moreover, the nonselectivity of **2** is in agreement with the high homology of the active sites of PTPs.

Amine fragment **3**, which accelerated the turnover of substrate **1** by MptpA phosphatase cooperatively as well as selectively, was selected for further validation. To quantify the observed enhancing effect, different concentrations of substrate **1** (0, 100, 200, 300, 400, 500, 750, and 1000 μM) were incubated with different concentrations of **3** (0–1000 μM), and the reactions were started by adding 0.3 μM MptpA in 50 mM Tris·HCl. The reactions were terminated by adding Malachite Green solution, and the amount of phosphate generated was determined. For each concentration of compound **3**, the initial rate of the enzymatic reaction, v_0, was plotted against the logarithm of the substrate concentration to provide an apparent K_M value (K_{Mapp}) for each of the fragment concentrations (Figure 2). Interestingly, the observed V_{max} values were not modified significantly at different concentrations of **3**, not even at the highest excess of **3** (Figure 2). From this observation it could be concluded that the k_{cat} value was not changed by

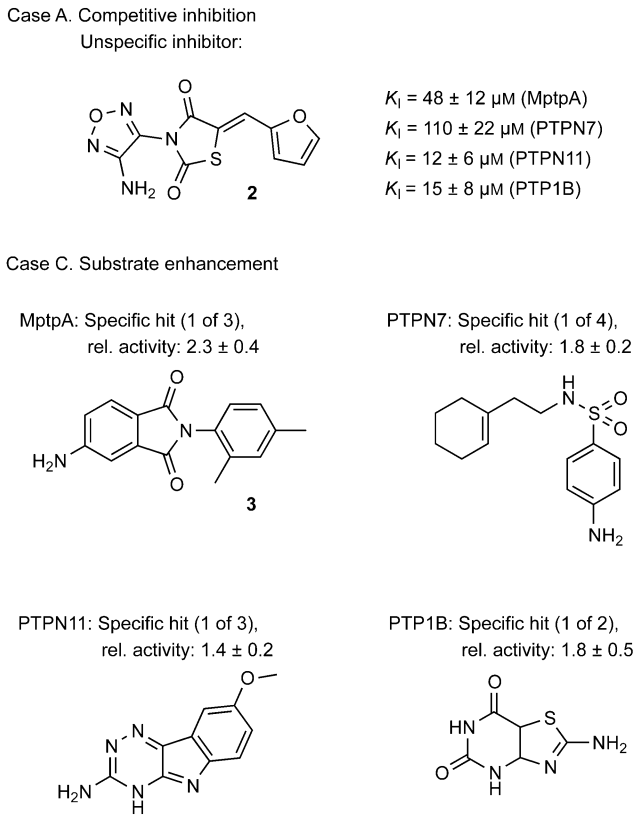

Scheme 1. Unspecific, competitive inhibitor **2** and specific, cooperative enhancer fragments were identified in ligation assays of substrate **1** with four different PTPs. K_I values were determined for inhibitor **2**. The effect of specific enhancing fragments is quantified by calculating the relative rate enhancement: (Abs_{630} with fragment + substrate − Abs_{630} blank)/(Abs_{630} without fragment − Abs_{630} blank).

varying the concentration of enhancing fragment **3** ($k_{cat} = V_{max}/[E]_t$). Therefore, the observed decrease in the apparent K_M values ($K_M = (k_{cat} + k_{-1})/k_1$) had to be a consequence of the increased binding affinity K_D ($K_D = k_{-1}/k_1$) of the ligation product to MptpA. This finding supported our hypothesis that **3** acted solely as a cooperative binder, increasing substrate affinity without accelerating the catalytic reaction itself. Similar correlations between inhibitor binding, K_I, and substrate conversion, K_M/k_{cat}, have been demonstrated previously for the phosphorus-containing peptide inhibitors of thermolysin, carboxypeptidase A, and pepsin.[22]

Finally, the apparent K_M values were analyzed as a function of the concentration of fragment **3**. While the K_M of **1** alone (K_{M1}) was 258.8 ± 29 μM, K_{Mapp} decreased with increasing concentrations of **3**. Fitting of the data with the reciprocal function

$$K_{Mapp}(F) = K_{M1} - \frac{K_{M1} - K_{M2}}{1 + K_M50/F}$$

indicated that K_{Mapp} approached a minimal, K_{M2}, at 104 ± 10 μM that was interpreted as being the K_{M2} of the ligation product **4**. The "K_M50 value", defined by a K_{Mapp} of $(K_{M1} + K_{M2})/2$, was 181.4 ± 19.5 μM; this indicated that the concentrations of free aldehyde substrate **1**, [A], and fragment ligation product (imine) **4**, [I], contributed equally to the overall phosphate generation at a total fragment concentration, $[F_t]$, of 181.4 μM and a total aldehyde concentration, $[A_t]$, of 181.4 μM. Considering the different K_M values of **1** and **4** and taking into account the unchanged k_{cat} value, this condition was reached at a ratio of concentrations [I]/[A] = 104/259. Inserting this ratio into the sum equation for the total aldehyde concentration $[A_t] = [A] + [I]$ resulted in the free aldehyde concentration [A] = 129.4 μM; insertion of this concentration into the sum equation for the total fragment concentration yielded the free fragment concentration [F] = 129.4 μM and [I] = 52 μM. The obtained concentrations finally indicated an equilibrium constant for the formation of the imine as

$$K_{eq} = \frac{[I]}{[A][F]} \frac{[\mathbf{4}]}{[\text{free } \mathbf{1}][\text{free } \mathbf{3}]} = 3.31\ \text{mM}^{-1}$$

in the presence of the protein.

For further confirmation, the postulated ligation product of **1** and **3** was converted into a potential inhibitor by replacing the phosphate ester with a phosphate mimic. Cooperative binder **3** was linked covalently with the phosphotyrosine mimetic *N*-(4-carboxyphenyl)trifluoromethylsulfonamide[23] (**5**) through an amide bond in **6** or through a reduced amide in **7**. Compounds **3**, **5**, **6**, and **7** were tested separately in functional enzyme assays based on *p*NPP and DiFMUP.[20] Phosphotyrosine mimetic **5** was equally active against all four PTPs, with a K_I value of approximately 300 μM (Scheme 2). In contrast, compounds **6** and **7** only showed activity towards MptpA with similar K_I values of 13 ± 6 μM (amide **6**) and 11 ± 7 μM (amine **7**). In agreement with the initial screening results for fragment **3**, compounds **6** and **7** showed no activity at a concentration of 300 μM against the other tested PTPs.

Molecular modeling of the protein–ligand complexes of **5** and **6** was performed in order to propose potential binding modes of the MptpA inhibitors. Two MptpA structures have been published, one contains a bound ligand (PDB ID: 1U2Q), the second is without a ligand (1U2P).[24] Compounds **5** and **6** were docked into the active site of the ligand-bound MptpA structure (1U2Q) by using AutoDock4. Phosphate mimetic **5** (magenta) in this model was able to bind direct with the catalytic residues of the protein (Figure 3A); compound **6** (blue) also fitted into the active site, as the overlay in Figure 3B shows, in addition, it was able to access a secondary binding site adjacent to the active pocket.

In summary, we have demonstrated the development of selective protein tyrosine phosphatase inhibitors based on the detection of cooperative, second-site binding fragments by dynamic substrate enhancement. Compounds **6** and **7** can compete well with the potency and selectivity of earlier MptpA inhibitors.[25–27]

Conclusion

The development of specific inhibitors of protein tyrosine phosphatases (PTP) has been hampered by the high similarity

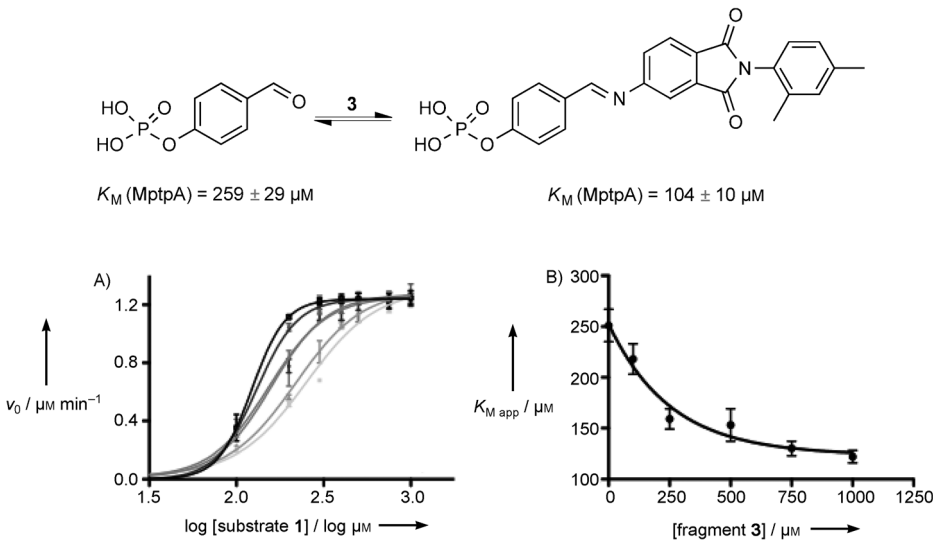

Figure 2. To determine the observed enhancing effect, various concentrations of substrate **1** were incubated with various concentrations of compound **3** (■: 0, ▲: 100, ▼: 250, ●: 500, ◆: 750, and ■: 1000 μM). After the reactions had been started by adding MptpA, A) initial velocities were recorded and B) apparent K_M values were obtained. The latter were plotted as a function of [**3**] and were used to determine the equilibrium of **3** and **1**. While the K_M value of **1** alone was 259 ± 29 μM, the apparent K_M as [**3**] increased approached the K_M of the ligation product **4** at 104 ± 10 μM. Nonlinear fitting of this saturation curve revealed a 50% value of the apparent K_M at a total fragment concentration of 181.4 μM, thus indicating equal contributions of substrates **1** and **4** to the phosphate release. Calculation yielded an equilibrium constant for the imine formation of K_{eq} = 3.31 mM^{-1} in the presence of the protein.

between the phosphotyrosine binding pocket of different PTPs. Addressing secondary binding sites might offer a solution to the problem. Here, specific PTP inhibitors were developed by a novel, fragment-based-ligation approach. Fragments that bind specifically to the secondary binding sites of four different PTPs were identified in a dynamic substrate-enhancement assay. A generic substrate for PTPs containing an aldehyde functionality was incubated together with one nucleophilic fragment per well and one phosphatase. The released inorganic phosphate was quantified by detecting its phosphomolybdate complex. The assay format can detect substrate-enhancing fragments that accelerate substrate cleavage and distinguish them from competitive inhibitors of the enzymes in the same set of experiments.

The mechanism of dynamic substrate enhancement was analyzed in greater detail for one selected fragment combination. The concentrations of the fragment and substrate were varied systematically, and the substrate turnover was monitored for each concentration. The enhancing fragment was found to increase the binding affinity of the generic substrate strongly, whereas it had no effect on the rate of the enzymatic reaction itself. The most strongly enhancing fragment was then converted into a PTP inhibitor by linking it irreversibly to a phosphotyrosine mimetic. The obtained inhibitor was fully selective for one of the four tested PTPs. In summary, the developed methodology should have significant potential for the fragment-based optimization of enzyme substrates and the fragment-based development of enzyme inhibitors. In principal, the method could be adapted to other enzymes, such as proteases, for which the conversion of substrates can be monitored in an enzyme assay. Although it had already been demonstrated that the screening of substrates can be successful in the definition of inhibitor structures, our approach allows a strongly facilitated variation of fragments by using the incubation of an electrophilic substrate with nucleophilic fragments.

Experimental Section

Materials and general methods: Commercially available reagents and solvents were obtained from Sigma Aldrich and used as received, unless otherwise noted. Reactions were monitored by analytical thin-layer chromatography on Merck silica gel 60 F524 plates. Compounds were visualized with a UV lamp. For HPLC analysis, an Agilent 1100 system was used with a reversed-phase column (Nucleosil 100 C-18, 5 μm, 2×250 mm (Grom, Herrenberg, Germany) operated with acetonitrile/water mixtures containing 0.1% formic acid), a diode array detector, and an ESI mass spectrometer employing single quadrupole detection. Microwave-assisted synthesis was performed on an Initiator Microwave Synthesizer from Biotage (Uppsala, Sweden). Bioassaying of PTPs was performed on a microtiter plate reader (UV absorption and fluorescence intensity: Safire^2, Tecan, Crailsheim, Germany). The protein tyrosine phosphatase (PTP) from *Mycobacterium tuberculosis* (MptpA) was isolated from a bacterial expression system in *E. coli*. Human PTPs (PTP1B, PTPN7, PTPN11) were provided by Prof. Dr. Stefan Knapp (University of Oxford, Structural Genomics Consortium).

Phosphoric acid mono-(4-formyl-phenyl) ester (1): Diethyl chlorophosphate (2.36 mL, 16.3 mmol, 1 equiv) was added dropwise to a cooled (0 °C) solution of 4-hydroxylbenzaldehyde (2 g, 16.3 mmol, 1 equiv) and triethylamine (2.3 mL, 19.6 mmol, 1.2 equiv) in dry CH_2Cl_2 under nitrogen. The reaction mixture was warmed to RT, and stirring was continued until completion of the reaction (3–6 h). The reaction mixture was extracted with HCl (1 M) and a saturated aqueous solution of Na_2CO_3. The organic phase was dried ($MgSO_4$) and concentrated in vacuo. A septum-sealed microwave tube charged with the protected phosphate (300 mg, 1.14 mmol, 1 equiv) and trimethylsilylbromide (300 μL, 2.3 mmol, 2 equiv) in CH_3CN was heated in the microwave synthesizer (60 °C, 10 min). After completion of the reaction, as indicated by TLC, the reaction mixture was quenched with MeOH/H_2O (95:5, *v/v*) and concentrated to give phosphate ester **1** in a yield of 3.0 g (91%). ^{1}H NMR (300 MHz, [D$_6$]DMSO): δ = 2.02 (br s, 2H; PO(OH)$_2$), 6.92 (d, J = 2 Hz, 2H; CH), 7.64 (d, J = 2 Hz, 2H; CH), 9.87 ppm (br s, 1H; CHO); ^{13}C NMR (75 MHz, [D$_6$]DMSO): δ = 116.4, 129.5, 131.3, 156.1, 191.0 ppm (CHO); ^{31}P NMR (121 MHz, [D$_6$]DMSO): δ = 22.3 ppm; ESI-MS: calcd for $C_7H_7O_5P$: 202.1 Da; found, *m/z* 201.1 Da $[M-H]^+$.

5-Amino-2-(2,4-dimethyl-phenyl)isoindole-1,3-dione (3): A septum-sealed microwave tube charged with 4-aminophthalic acid

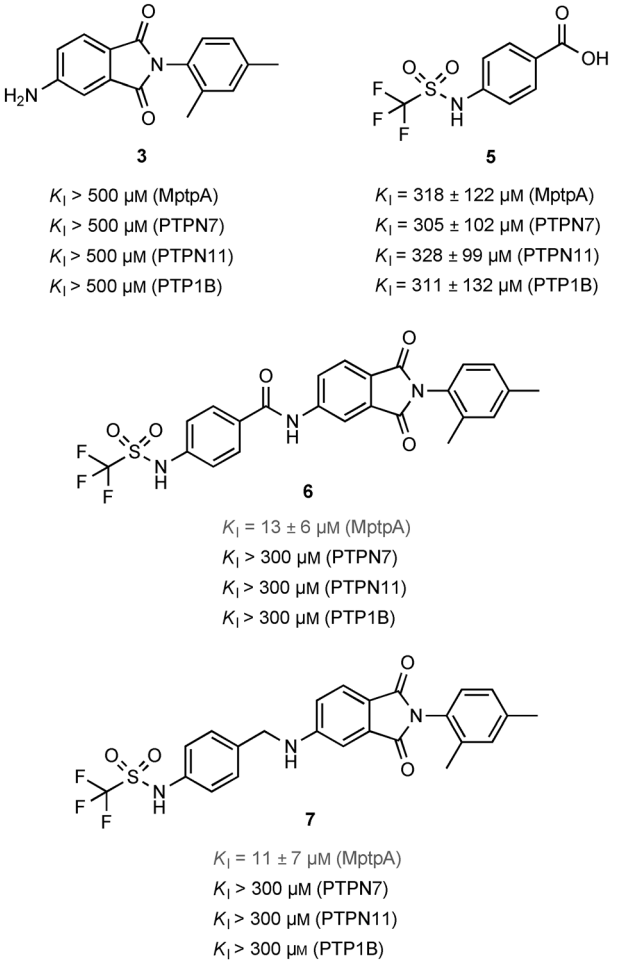

Scheme 2. Inhibitor development starting from the enhancing fragment **3** and the phosphotyrosine isoster fragment **5**. Irreversible fragment condensation products **5** and **6** are specific inhibitors of MptpA in preference to the other three tested PTPs.

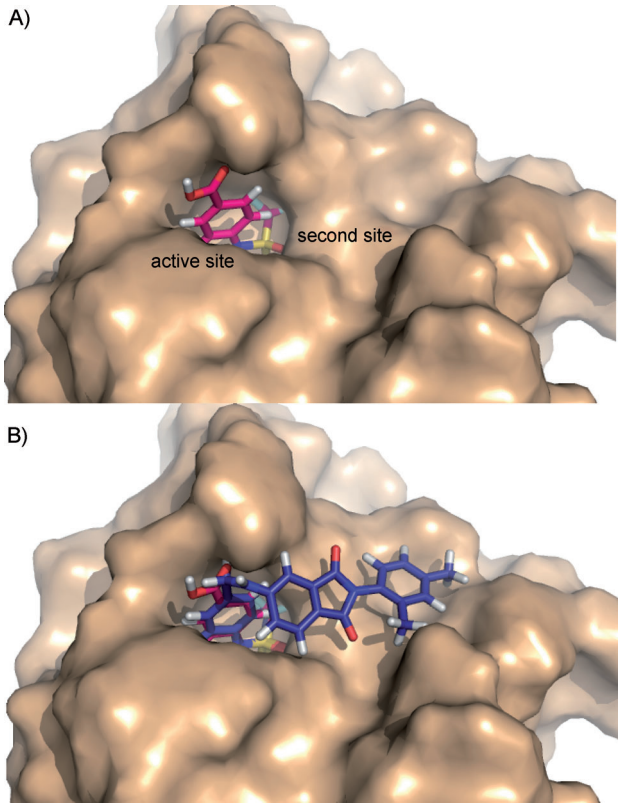

Figure 3. A) Model of 4-(trifluoromethanesulfonylamino)benzoic acid **5** (magenta) binding into the active site of MptpA. B) Overlay of **5** (magenta) and **7** (blue) using AutoDock4 with AutoDockTools indicating that **7** addresses the active site and the potential second site docked in MptpA (1U2Q). The structural data suggest that a secondary binding site next to the phosphotyrosine binding site exists and can be used for selective PTP inhibitor design. The figures were generated with PyMOL v.0.99.[29]

(200 mg, 1.1 mmol, 1 equiv), 2,4-dimethylphenylamine (1.36 mL, 11 mmol, 10 equiv), and triethylamine (1.53 mL, 11 mmol, 10 equiv) was heated in a microwave (160 °C, 30 min). After completion of the reaction, as indicated by TLC, the reaction mixture was concentrated and purified by column chromatography (toluene/acetone 4:1, *v/v*) to yield 228.5 mg of compound **3** (78%). ^{1}H NMR (300 MHz, [D$_6$]DMSO): δ = 2.10 (s, 3H; CH$_3$), 2.25 (s, 3H; CH$_3$), 4.60 (br s, 2H; NH$_2$), 6.79 (d, J = 3 Hz, 1H; CH), 7.04 (d, J = 2 Hz, 1H; CH), 7.08 (s, 1H; CH), 7.25 (s, 1H; CH), 7.45 ppm (m 2H; CH); ^{13}C NMR (75 MHz, [D$_6$]DMSO): δ = 17.75, 20.75 (CH$_3$), 115.23, 115.81, 119.28, 121.16, 121.83, 123.37, 126.75, 131.32, 131.55, 132.12, 143.67 (C–N), 153.26 (C–NH$_2$), 166.04, 167.06 ppm (CO); ESI-MS: calcd for $C_{16}H_{14}N_2O_2$: 266.29 Da; found: *m/z* 267.0 Da $[M-H]^+$.

4-(Trifluoromethylsulfonylamido)benzoic acid (5): 4-Aminobenzoic acid methyl ester (1 g, 6.7 mmol, 1 equiv) and pyridine (540 μL, 6.7 mmol, 1 equiv) were dissolved in CH_2Cl_2 (150 mL) under nitrogen, and the mixture was cooled to 0 °C. Trifluoromethanesulfonic anhydride (5.96 mL, 35 mmol, 5 equiv) was added dropwise. The reaction mixture was stirred overnight, warmed up to room temperature, and extracted with 5% HCl and H_2O. The organic phase was dried ($MgSO_4$) and concentrated in vacuo. The obtained material was dissolved in LiOH (50 mL, 0.1 M), and the mixture was stirred for 1 h. Ion exchanger was added, and the reaction mixture was stirred until neutral pH was reached, then lyophilized from acetonitrile/water to yield 1.71 g of compound **5** (95%). ^{1}H NMR (300 MHz, [D$_6$]DMSO): δ = 7.61 (m, 2H; CH), 7.95 (m, 2H; CH), 10.61 ppm (br s, 1H; COOH); ^{13}C NMR (75 MHz, [D$_6$]DMSO): δ = 106.21, 110.39, 114.56, 123.62 (CF$_3$), 121.19, 121.92, 133.74, 144.10 (Ar), 169.80 ppm (COOH); ESI-MS: calcd for $C_8H_6F_3NO_4S$: 269.2 Da; found: *m/z* 268.2 Da $[M-H]^+$.

***N*-[2-(2,4-Dimethyl-phenyl)-1,3-dioxo-2,3-dihydro-1*H*-isoindol-5-yl]-4-(trifluoromethylsulfonamido)benzamide (6)**: 4-(Trifluoromethanesulfonylamino)benzoic acid (**5**) (50 mg, 0.19 mmol, 1 equiv) was dissolved in dry CH_2Cl_2 (5 mL). Thionyl chloride (140 μL, 1.6 mmol, 10 equiv) was added dropwise, and the solution was stirred at 60 °C for 6 h. Solvents were evaporated, and the residue was resolved in CH_2Cl_2. This procedure was repeated three times. After complete evaporation of thionyl chloride, the product, 4-trifluoromethane sulfonylamino benzoyl chloride, was dissolved in CH_2Cl_2 (2 mL) under nitrogen. 5-Amino-2-(2,4-dimethyl-phenyl)isoindole-1,3-dione (**2**, 61 mg, 0.23 mmol, 1.2 equiv) and pyridine (19 μL, 0.23 mmol, 1.2 equiv) were dissolved in dry CH_2Cl_2 (1 mL). The resulting solution was added dropwise to the solution of the acyl chloride. The reaction mixture was stirred overnight, then the solvents were evaporated. Product **6** was purified by preparative HPLC in a yield of 42.3 mg (43%). ^{1}H NMR (300 MHz [D$_6$]DMSO): δ = 2.12 (s, 3H; CH$_3$), 2.32 (s, 3H; CH$_3$), 7.01 (m, 1H; CH), 7.27 (m, 1H; CH), 7.81 (m, 4H; CH), 7.94 (m, 1H; CH), 8.14 (m, 1H; CH), 8.37 ppm (m, 1H; CH); ^{13}C NMR (75 MHz [D$_6$]DMSO): δ = 17.83,

20.98, 100.72, 108.66, 115.93, 116.73, 120.08, 121.22, 122.32, 124.82, 125.32, 125.59, 126.82, 128.19, 131.34, 131.78, 132.70, 142.33, 144.68, 165.81 (CONH), 166.10 (CO), 167.03 ppm (CO); ESI-MS: calcd for $C_{24}H_{18}F_3N_3O_5S$: 517.5 Da; found: *m/z* 518.5 Da $[M+H]^+$.

***N*-(4-((2-(2,4-Dimethyl-phenyl)-1,3-dioxo-1,3-dihydro-1*H*-isoindol-5-yl)amino-methyl)phenyl)trifluoromethyl-sulfonamide (7)**: A septum-sealed microwave tube charged with 4-(4-trifluoromethylsulfonylamino-benzylamino)phthalic acid (10 mg, 24 μmol, 1 equiv), 2,4-dimethylaniline (30 μL, 240 μmol, 10 equiv), and triethylamine (34 μL, 240 μmol, 10 equiv) was irradiated in the microwave (160 °C, 30 min). After completion of the reaction, as indicated by TLC, the reaction mixture was concentrated and purified by preparative HPLC to yield 14.6 mg of **7** (78%). ^{1}H NMR (300 MHz, [D$_6$]DMSO): $\delta = 2.13$ (s, 3H; C*H*$_3$), 2.28 (s, 3H; C*H*$_3$), 4.24 (s, 2H; C*H*$_2$), 7.05 (m, 7H; C*H*), 7.29 (m, 2H; C*H*), 7.58 ppm (m, 1H; C*H*); ^{13}C NMR (75 MHz, [D$_6$]DMSO): $\delta = 17.78$, 20.82, 50.92, 100.67, 109.72, 115.69, 116.59, 118.98, 120.72, 121.16, 124.13, 124.51, 126.83, 128.89, 131.59, 134.88, 135.47, 137.59, 145.73, 151.45, 166.09 (CO), 167.04 ppm (CO); ESI-MS: calcd for $C_{24}H_{20}F_3N_3O_4S$: 503.5 Da; found: *m/z* 504.5 Da $[M+H]^+$.

Malachite Green assay for the determination of phosphate (P_i): The color reagent for orthophosphate determination was prepared as previously described.[14] Concentrated sulfuric acid (60 mL, $d = 1.84\ g\,L^{-1}$) was slowly added to water (300 mL). The solution was then cooled to room temperature and supplemented with Malachite Green (0.44 g). The resulting orange solution is stable for at least one year at room temperature. On the day of use, 7.5% ammonium molybdate (2.5 mL) was added to the dye solution (10 mL) along with 11% Tween20 (0.2 mL) and water (19.05 mL). Finally, this solution (70 μL) was added to the phosphate-containing reaction mixture (20 μL). Assays were performed in untreated, clear, 384-well microtiter plates (Corning B.V. Life Sciences, Schipol-Rijk, The Netherlands). All experiments were performed on microplate reader Safire^2 (Tecan). Tris·HCl buffer (50 mM, pH 7.0) was used. A standard curve was measured to determine the correlation between absorption and phosphate (P_i) concentration with $\varepsilon = 12195\ M^{-1}cm^{-1}$. Assay conditions were validated specifically for each of the four protein tyrosine phosphatases. After the amine diversity subset had been screened against the PTP of interest, the identified primary hit compounds (inhibitors and activators) were validated under the same condition in replicate measurements.

Composition of a fragment library for screening: 110 primary amines were selected from the FMP ChemBioNet library by diversity considerations. The members of the ChemBioNet library were selected by the recently reported maximum common-substructure concept (MCS).[19]

MptpA: The kinetic parameters of MptpA were determined by plotting several substrate concentrations against measured activity. A K_M of 259 ± 29 μM, a V_{max} of 1.311 ± 0.051 μM min^{-1}, and a k_{cat} of 4.37 ± 0.17 min^{-1} were determined at an enzyme concentration of 0.3 μM after end-point measurements ($t_{incubation} = 30$ min). To screen MptpA (0.3 μM), substrate **1** (250 μM) and nucleophilic fragment (500 μM) in Tris·HCl (50 mM, pH 7; total volume 20 μL) were incubated for 60 min. Then the Malachit Green solution (70 μL) was added.

PTPN7: The kinetic parameters of PTPN7 were determined by plotting several substrate concentrations against measured activity. A K_M of 266 ± 96 μM, a V_{max} of 3.437 ± 0.56 μM min^{-1}, and a k_{cat} of 11.4 ± 1.9 min^{-1} were determined at an enzyme concentration of 0.3 μM after end-point measurements ($t_{incubation} = 60$ min). To screen PTPN7 (0.3 μM), substrate **1** (250 μM) and nucleophilic fragment (500 μM) in Tris·HCl (50 mM, pH 7; total volume 20 μL) were incubated for 60 min. Then the Malachit Green solution (70 μL) was added.

PTPN11: The kinetic parameters of PTP11 were determined by plotting several substrate concentrations against measured activity. A K_M of 613 ± 256 μM, a V_{max} of 4.406 ± 1.157 μM min^{-1}, and a k_{cat} of 25.9 ± 6.8 min^{-1} were determined at an enzyme concentration of 0.17 μM after end-point measurements ($t_{incubation} = 60$ min). To screen PTPN11 (0.17 μM), substrate **1** (250 μM) and nucleophilic fragment (500 μM) in Tris·HCl (50 mM, pH 7; total volume 20 μL) were incubated for 60 min. Then the Malachit Green solution (70 μL) was added.

PTP1B: The enzyme kinetic parameters of PTP1B were determined by plotting several substrate concentrations against measured activity. A K_M of 319 ± 57 μM, a V_{max} of 9.135 ± 0.800 μM min^{-1}, and a k_{cat} of 6.5 ± 0.6 min^{-1} were determined at an enzyme concentration of 1.4 μM after end-point measurements ($t_{incubation} = 15$ min). To screen PTP1B (1.4 μM), substrate **1** (250 μM) and nucleophilic fragment (500 μM) in Tris·HCl (50 mM, pH 7; total volume 20 μL) were incubated for 15 min. Then the Malachit Green solution (70 μL) was added.

Quantification and characterization of the enhancing effect: Substrate **1** (0, 100, 200, 300, 400, 500, 750, and 1000 μM) was incubated with different concentrations of amine **3** (0, 100, 250, 500, 750, and 1000 μM) in Tris·HCl (50 mM, pH 7); the reactions were started by adding MptpA (0.3 μM) resulting in a total volume of 20 μL. The reactions were terminated after 30 min by adding Malachite Green solution (70 μL) in order to determine the final concentration of phosphate. For each concentration of compound **3**, the initial rate of the enzymatic reaction, v_0, was plotted against the logarithm of the substrate concentration to provide an apparent K_M value (K_{Mapp}) for each of the fragment concentrations (Figure 2).

While the K_M value of **1** alone was 259 ± 29 μM, K_{Mapp} at increasing concentrations of **3** approached 104 ± 10 μM, which can be interpreted as the K_M value of the ligation product. Nonlinear fitting of this saturation curve by employing GraphPad Prism 4 for Windows indicated that the 50% value of K_{Mapp} was reached at a total fragment concentration of 181.4 μM; at this concentration 50% of the substrate turnover was contributed by each of the two species.

Enzymatic phosphatase assays: PTP activity was determined in 384-well microtiter plates by using 4-nitrophenyl phosphate (*p*NPP) and 6,8-difluoro-4-methyl-umbelliferyl phosphate (DiFMUP)[20] as substrates and the microtiter plate reader Safire^2 (Tecan). Tris·HCl (50 mM), NaCl (150 mM), and DTT (1 mM) were used as buffer conditions. To determine the K_i values of identified compounds, inhibitors (0, 10, 25, 50, 100, 250, 500 μM) were incubated in triplicate with the PTP of interest (0.3 μM MptpA, 0.3 μM PTPN7, 0.1 μM PTPN11, 1 μM PTP1B) and *p*NPP (10 mM) or DiFMUP (10 μM) in a total volume of 20 μL. The obtained average data were plotted in an Excel sheet so as to determine K_i values by nonlinear regression fittings, as previously described.[28]

Molecular Modeling: Molecular modeling was performed by using AutoDock 4 with AutoDockTools (http://autodock.scripps.edu). Two crystal structures of MptpA are available from the Protein Data Bank (http://www.pdb.org). One with (PDB ID: 1U2Q) and one without (1U2P) a bound ligand.[24] Compounds **5** and **6** were docked into the active site of the 1U2Q MptpA structure. The PDB receptor file 1U2Q was edited by AutoDockTools. All water molecules were removed, and hydrogen atoms were added. The file was saved as a PDBQT file. In parallel, PDBQT ligand files were pre-

pared. Afterwards a grid parameter file (GPF) was generated that focused on the phosphotyrosine binding pocket of MptpA. Finally, the docking parameter file (DPF) was prepared. The docking parameters recommended in the tutorial (*Using AutoDock 4 with AutoDockTools: A Tutorial*) were adapted. Genetic algorithm with local search (GALS), also known as the Lamarckian genetic algorithm, was selected as docking algorithm. The figures were generated and rendered with PyMOL v.0.99.[29]

Acknowledgements

We thank Swantje Behnken, Dr. Samuel Beligny, Dr. Jörn Saupe, and Carola Seyffarth for technical assistance and fruitful discussions, the DFG (SFB 765, FOR 806, Ra 895/2-5) and the Fonds der Chemischen Industrie for financial support, and Prof. Stefan Knapp and Dr. Alastair Barr (Structural Genomics Consortium, University of Oxford) for providing PTPs.

Keywords: drug discovery · dynamic ligation assay · *Mycobacterium tuberculosis* · protein tyrosine phosphatases · second-site binders

[1] T. Hunter, *Cell* **2000**, *100*, 113 – 127.
[2] A. Alonso, J. Sasin, N. Bottini, I. Friedberg, I. Friedberg, A. Osterman, A. Godzik, T. Hunter, J. Dixon, T. Mustelin, *Cell* **2004**, *117*, 699 – 711.
[3] O. M. Fischer, S. Streit, S. Hart, A. Ullrich, *Curr. Opin. Chem. Biol.* **2003**, *7*, 490 – 495.
[4] M. E. Noble, J. A. Endicott, L. N. Johnson, *Science* **2004**, *303*, 1800 – 1805.
[5] L. Bialy, H. Waldmann, *Angew. Chem.* **2005**, *117*, 3880 – 3906; *Angew. Chem. Int. Ed.* **2005**, *44*, 3814 – 3839.
[6] A. K. H. Hirsch, F. R. Fischer, F. Diederich, *Angew. Chem.* **2007**, *119*, 342 – 357; *Angew. Chem. Int. Ed.* **2007**, *46*, 338 – 352.
[7] M. A. T. Blaskovich, *Curr. Med. Chem.* **2009**, *16*, 2095 – 2176.
[8] A. J. Barr, E. Ugochukwu, K. W. Lee, O. N. King, P. Filippakopoulos, I. Alfano, P. Savitsky, N. A. Burgess-Brown, S. Müller, S. Knapp, *Cell* **2009**, *136*, 352 – 363.
[9] A. Ciulli, C. Abell, *Curr. Opin. Biotechnol.* **2007**, *18*, 489 – 496.
[10] M. F. Schmidt, J. Rademann, *Trends Biotechnol.* **2009**, *27*, 512 – 521.
[11] M. F. Schmidt, A. Isidro-Llobet, M. Lisurek, A. El-Dahshan, J. Tan, R. Hilgenfeld, J. Rademann, *Angew. Chem.* **2008**, *120*, 3319 – 3323; *Angew. Chem. Int. Ed.* **2008**, *47*, 3275 – 3278.
[12] M. F. Schmidt, A. El-Dahshan, S. Keller, J. Rademann, *Angew. Chem.* **2009**, *121*, 6464 – 6467; *Angew. Chem. Int. Ed.* **2009**, *48*, 6346 – 6349.
[13] M. B. Soellner, K. A. Rawls, H. Tsuruoka, R. K. Jain, J. A. Ellman, *J. Am. Chem. Soc.* **2007**, *129*, 9613 – 9615.
[14] A. A. Baykov, O. A. Evtushenko, S. M. Avaeva, *Anal. Biochem.* **1988**, *171*, 266 – 270.
[15] H. Bach, K. G. Papavinasasundaram, D. Wong, Z. Hmama, Y. Av-Gay, *Cell Host Microbe* **2008**, *3*, 316 – 322.
[16] M. Elchebly, P. Payette, E. Michaliszyn, W. Cromlish, S. Collins, A. L. Loy, D. Normandin, A. Cheng, J. Himms-Hagen, C.-C. Chan, C. Ramachandran, M. J. Gresser, M. L. Tremblay, B. P. Kennedy, *Science* **1999**, *283*, 1544 – 1548.
[17] B. Zanke, J. Squire, H. Griesser, M. Henry, H. Suzuki, B. Patterson, M. Minden, T. W. Mak, *Leukemia* **1994**, *8*, 236 – 244.
[18] K. Hellmuth, S. Grosskopf, C. T. Lum, M. Würtele, N. Röder, J. P. von Kries, M. Rosario, J. Rademann, W. Birchmeier, *Proc. Natl. Acad. Sci. USA* **2008**, *105*, 7275 – 7280.
[19] M. Lisurek, B. Rupp, J. Wichard, M. Neuenschwander, J. P. von Kries, R. Frank, J. Rademann, R. Kühne, *Mol. Diversity* **2010**, *14*, 401 – 408.
[20] L. Tautz, T. Mustelin, *Methods* **2007**, *42*, 250 – 260.
[21] R. Maccari, R. Ottanà, R. Ciurleo, P. Paoli, G. Manao, G. Camici, C. Laggner, T. Langer, *ChemMedChem* **2009**, *4*, 957 – 962.
[22] M. M. Mader, P. A. Bartlett, *Chem. Rev.* **1997**, *97*, 1281 – 1301.
[23] a) S. Großkopf, J. Rademann, unpublished results; b) P. Huang, J. Ramphal, J. Wei, C. Liang, B. Jallal, G. McMahon, C. Tang, *Bioorg. Med. Chem.* **2003**, *11*, 1835 – 1849.
[24] C. Madhurantakam, E. Rajakumara, P. A. Mazumdar, B. Saha, D. Mitra, H. G. Wiker, R. Sankaranarayanan, A. K. Das, *J. Bacteriol.* **2005**, *187*, 2175 – 2181.
[25] M. Manger, M. Scheck, H. Prinz, J. P. von Kries, T. Langer, K. Saxena, H. Schwalbe, A. Fuerstner, J. Rademann, H. Waldmann, *ChemBioChem* **2005**, *6*, 1749 – 1753.
[26] L. D. Chiaradia, A. Mascarello, M. Purificação, J. Vernal, M. N. S. Cordeiro, M. E. Zenteno, A. Villarino, R. J. Nunes, R. A. Yunes, H. Terenzi, *Bioorg. Med. Chem. Lett.* **2008**, *18*, 6227 – 6230.
[27] K. A. Rawls, P. T. Lang, J. Takeuchi, S. Imamura, T. D. Baguley, C. Grundner, T. Alber, J. A. Ellman, *Bioorg. Med. Chem. Lett.* **2009**, *19*, 6851 – 6854.
[28] G. Kemmer, S. Keller, *Nat. Protoc.* **2010**, *5*, 267 – 281.
[29] W. L. DeLano, *The PyMOL Molecular Graphics System*, *v.0.99*, DeLano Scientific, San Carlos, **2002**.

Received: June 27, 2011
Published online on November 3, 2011

